Origin of the High Néel Temperature in $SrTcO_3$

Jernej Mravlje,[1,2,3] Markus Aichhorn,[4] and Antoine Georges[2,1,5]

[1]*Collège de France, 11 place Marcelin Berthelot, 75005 Paris, France*
[2]*Centre de Physique Théorique, École Polytechnique, CNRS, 91128 Palaiseau Cedex, France*
[3]*Jožef Stefan Institute, Jamova 39, Ljubljana, Slovenia*
[4]*Institute of Theoretical and Computational Physics, TU Graz, Petersgasse 16, Graz, Austria*
[5]*DPMC, Université de Genève, 24 quai Ernest Ansermet, CH-1211 Genève, Switzerland*

(Received 4 August 2011; published 8 May 2012; corrected 18 May 2012)

We investigate the origin of the high Néel temperature recently found in Tc^{4+} perovskites. The electronic structure in the magnetic state of $SrTcO_3$ and its $3d$ analogue $SrMnO_3$ is calculated within a framework combining band-structure and many-body methods. In agreement with experiment, for $SrTcO_3$ a smaller magnetic moment and 4 times larger Néel temperature are found. We show that this is because the Tc compound lies on the verge of the itinerant-to-localized transition, while the Mn compound lies deeper into the localized side. For $SrTcO_3$ we predict that the Néel temperature depends weakly on applied pressure, in clear violation of Bloch's rule, signaling the complete breakdown of the localized picture.

DOI: 10.1103/PhysRevLett.108.197202 PACS numbers: 75.47.Lx, 71.27.+a, 75.50.Ee

Recently, antiferromagnetism persisting to very high temperatures exceeding 1000 K has been reported for $SrTcO_3$ [1,2] and other Tc^{4+} perovskites [3]. Because Tc is a radioactive element, those perovskites have been scarcely investigated, and for many of them only structural properties are known. This discovery is especially striking, since robust magnetism with high transition temperatures has been reported up to now only for $3d$ transition metals and their oxides, which realize large moments in localized $3d$ shells. Indeed, magnetism in $4d$ materials with more extended orbitals has been rarely found. Among the few reported cases, the antiferromagnetic Ca_2RuO_4 has a low Néel temperature of 110 K [4], and $SrRuO_3$ is an itinerant ferromagnet with $T_c = 160$ K and a small moment about $1.5\mu_B$ [5,6].

The Néel temperature of $SrTcO_3$ appears remarkably high especially when compared to $T_N = 260$ K [7] found in its $3d$ analogue $SrMnO_3$. The comparison is in order, as both compounds have the same G-type antiferromagnetic order and adopt a simple cubic structure in the relevant temperature range. Remarkably, the Tc magnetic moment found is smaller, $2.1\mu_B$ [1], compared to $2.6\mu_B$ [7] for the Mn compound. In Ref. [1], the small Tc moment is attributed to covalency [8], that is, to the moment residing in orbitals with considerable weight on oxygen sites, where it overlaps with the opposite moment of the neighboring Tc atom. However, the covalency is large in the electronic structure of $SrMnO_3$ as well [9] and thus cannot explain the smaller moment or the much higher Néel temperature [1] of the Tc compound.

In this Letter, we resolve this puzzling situation by calculating the electronic structure of $SrTcO_3$ and $SrMnO_3$ in a theoretical framework which combines band-structure and many-body methods, as appropriate for d shells with strong correlations. Our approach allows us to put forward qualitative explanations, which we support by quantitative calculations. First, we point out that Tc^{4+} compounds are unique among $4d$ oxides: Because they have a half-filled t_{2g} shell, the moderate Coulomb repulsion associated with extended $4d$ orbitals is nevertheless sufficient to localize the electrons. Second, we show that the key property of $SrTcO_3$ is that it is located close to the metal-insulator transition of the paramagnetic state and that the Néel temperature is maximal there, as anticipated in Ref. [10]. In contrast, $SrMnO_3$ is deeper into the insulating side. Third, we relate the smaller magnetic moment in $SrTcO_3$ to the corresponding larger charge fluctuations in this compound. The effects of covalency with oxygen are carefully analyzed as well.

The authors of Ref. [1] recognized the more itinerant nature of $SrTcO_3$ but still based their explanation of magnetism on a large Heisenberg exchange interaction J_H, a point of view forcefully advocated in Ref. [11]. Under pressure, J_H increases and most oxides obey Bloch's rule [12], $\alpha = d\log(T_N)/d\log V \approx -3.3$. We demonstrate that, for $SrTcO_3$, a small value of α is found, hence violating Bloch's rule. This is a hallmark of $SrTcO_3$ being at the verge of an itinerant-to-localized transition and signals the inapplicability of the localized description.

Methods.—We use the theoretical framework which combines dynamical mean-field theory (DMFT) and density-functional theory in the local density approximation (LDA), in the charge self-consistent implementation of Refs. [13,14] based on the WIEN2K package [15]. The cubic crystal structure and G-type antiferromagnetic unit cell have been used for both compounds. Wannier t_{2g} orbitals ψ_m are constructed out of Kohn-Sham bands within the energy window containing t_{2g} bands, that is, within $[-2.5, 1.2]$ and $[-2.0, 0.8]$ eV for Tc and Mn compounds, respectively. We use a fully rotationally invariant

interaction in the form $H_I = (U - 3J)n(n-1)/2 - 2JS^2 - 1/2JT^2$, with U the on-site Hubbard interaction, J Hund's rule coupling, and n, S, and T the total charge, spin, and orbital momentum on the atom, respectively. We solve the DMFT quantum impurity problem by using the TRIQS toolkit [16] and its implementation of the continuous-time quantum Monte Carlo algorithm [17,18]. The interaction parameters were chosen as $U = 2.3$ eV, $J = 0.3$ eV for Tc and $U = 3.5$ eV, $J = 0.6$ eV for Mn compound. For the former, we set the parameters close to the values of the Ru compounds [19]. For the latter, we checked that the position of the lower Hubbard band agrees reasonably well with photoemission spectroscopy [20]. The results do not change significantly if the interaction parameters are varied in the physically plausible range. For $SrMnO_3$ we checked also that the e_g degrees of freedom are inactive by performing a 5-orbital calculation including e_g orbitals. The magnetization found then is indistinguishable from the results reported below using only t_{2g} states. To account for the covalency effects, the magnetic moment is recalculated also with a different choice of Wannier orbitals Ψ_m constructed from the larger energy window including all the oxygen bands.

Results.—Our main result accounting for the key qualitative aspects reported in experiments is presented in Fig. 1. Because all spatial fluctuations are neglected in DMFT, which is a mean-field approach, the absolute magnitude of the calculated Néel temperature exceeds the real values by about a factor of 2, as documented in previous work [21]. The magnetic moments are thus plotted vs the temperature of the simulation halved. The staggered moment (solid lines) decreases with increasing temperature and vanishes at a Néel temperature which is about 4 times larger for the Tc compound, in agreement with experiments. Also in agreement with experiment, the Tc magnetic moment is smaller. The plotted magnetic moments are calculated from the magnetization on the orbitals ψ_m by $\mu = \mu_B \sum_m [n_\uparrow(\psi_m) - n_\downarrow(\psi_m)]$, where $n_\sigma(\psi)$ is the density of electrons on orbital ψ with spin σ. Because these orbitals have considerable weight on the oxygen ions, the low-temperature moments exceed experimental values by about 15%. These Wannier orbitals are deliberately chosen to stress that the suppression of the magnetic moment on Tc is not due to covalency effects alone. The quantitatively correct low-temperature moments are reported towards the end of this Letter.

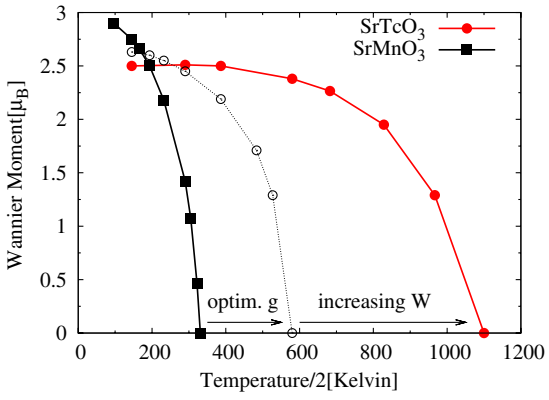

FIG. 1 (color online). Solid lines: Temperature dependence of $SrTcO_3$ (filled circles) and $SrMnO_3$ (squares) "Wannier" magnetic moments in orbitals ψ_m (see discussion in the text). Note that the x axis has been rescaled due to systematic overestimation of T_N in DMFT [21]. Open circles: Results obtained for a hypothetical compound having the $SrMnO_3$ band structure but artificially reduced interactions yielding a maximal Néel temperature.

In Fig. 2, we plot the total and orbitally resolved paramagnetic LDA density of states (DOS). Both materials have three t_{2g} electrons, with the t_{2g} manifold at the Fermi level, oxygen states below, and e_g states above. The t_{2g} bands constructed out of Tc $4d$ orbitals are considerably broader with a bandwidth $W \approx 3.6$ eV, compared to 2.3 eV found in $3d$ Mn. Covalency, as measured by comparing the oxygen weight in the t_{2g} energy window, is significant in both compounds: The integrated oxygen DOS amounts to about 20% of the total integrated DOS for both cases. Once due to the correlations the e_g states are pushed to higher energies, both compounds have a half-filled t_{2g} shell with a low lying $S = 3/2$ multiplet. Among $4d$ perovskites, in which e_g-t_{2g} crystal field splitting exceeds Hund's rule coupling, this largest possible spin is realized only in the Tc compounds, since other elements (Ru and Mo) are not stable in the appropriate oxidation state. In the inset, the LDA + DMFT t_{2g} DOS is plotted. The correlations open up a gap of 1 eV, a bit smaller than 1.5 eV found in hybrid-functional calculations [11]. The gap in the local spin density approximation (LSDA) is 0.3 eV [1].

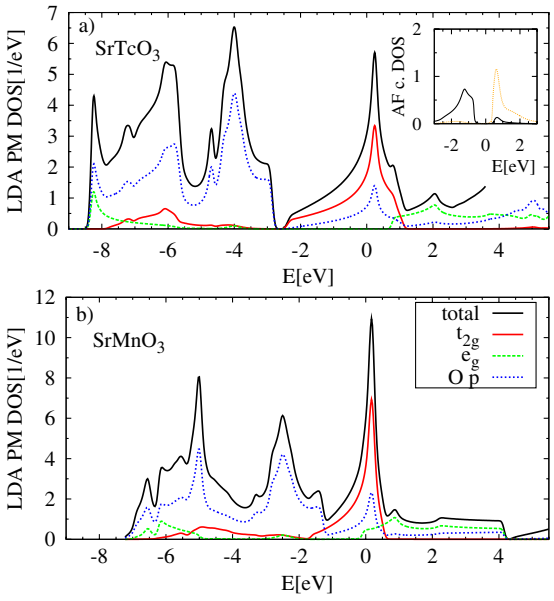

FIG. 2 (color online). The total and orbitally resolved LDA paramagnetic (PM) DOS for (a) $SrTcO_3$ and (b) $SrMnO_3$. Inset: Predicted spin-resolved LDA + DMFT DOS.

While their large spin gives a hint about why Tc perovskites are special among 4*d* oxides, it does not tell why their 3*d* analogue $SrMnO_3$ has a Néel temperature which is 4 times smaller. To understand this, we first turn to qualitative considerations. In the localized picture, antiferromagnetism can be described in terms of the Heisenberg model: $H = J_H \sum_{\langle ij \rangle} \mathbf{S}_i \cdot \mathbf{S}_j$. The superexchange coupling J_H between neighboring spins $\mathbf{S}_i$ and $\mathbf{S}_j$ appears due to the optimization of kinetic energy of the underlying itinerant model and thus scales as $W^2/\mathcal{U}$, where W is the bandwidth and $\mathcal{U}$ measures the strength of the Coulomb interaction. On the other hand, starting from the itinerant side the magnetism can be described within a mean-field treatment of electronic interactions. When perfect nesting applies, this treatment yields an exponentially small gap and transition temperature $\propto \exp(-W/\mathcal{U})$. Hence, a key observation is that robust magnetism occurs at intermediate values of interaction $\mathcal{U} \approx W$ where the crossover from the itinerant regime to the local regime takes place. This has been established firmly for the half-filled 3*d* Hubbard model, where the largest Néel temperature T_N is found very close to the metal-insulator transition (MIT) in the paramagnetic state [22] (cf. gray line in Fig. 3).

To relate this qualitative discussion to the realistic multiorbital cases at hand, we calculated the properties of two compounds for a range of fictitious interaction parameters. The J/U values are fixed to 0.17 and 0.13 for the Mn and Tc band structure, respectively. A larger J/U value for 3*d* compounds is used since the oxygen bands are closer for 3*d*'s and screen U more efficiently than J. We denote the energy of the lowest atomic excitation of $S = 3/2$ atomic

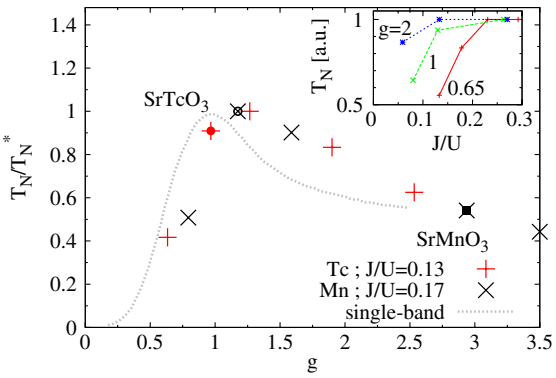

FIG. 3 (color online). The Néel temperatures as a function of coupling $g \equiv \mathcal{U}/\mathcal{U}_c$, with $\mathcal{U} \equiv U + 2J$ and $\mathcal{U}_c = (U + 2J)_c$ the value at which the MIT in the paramagnetic state occurs. T_N are normalized to the maximum Néel temperature T_N^* found when varying $\mathcal{U}$. The gray line is for the single-band Hubbard model (DMFT calculation of Ref. [22]). The full circle and square indicate the data at the physical value of interaction for the band structure of the Tc and Mn compound, respectively. The empty circle denotes data for the Mn compound but artificially reduced interaction; see Fig. 1. Inset: The dependence of T_N on J/U at few g.

ground state by $\mathcal{U} = U + 2J$. $\mathcal{U}$ is the relevant quantity for estimating where the system is located in the phase diagram with respect to the MIT, and the Mott gap is $\mathcal{U} - cW$, where c is of the order of unity. The MIT in the paramagnetic state occurs at a critical value $\mathcal{U} = \mathcal{U}_c$, where $\mathcal{U}_c = 3.0$ eV ($U = 2.4$ eV) for Tc and $\mathcal{U}_c = 1.6$ eV ($U = 1.2$ eV) for Mn, the larger $\mathcal{U}$ for Tc being due to the larger bandwidth. While the physical value of U for Tc is close to the value at which the transition takes place [1,10], Mn is situated further to the insulating side. For non-half-filled t_{2g}'s, the critical $\mathcal{U}_c$ is increased by $5J$ [23], so that most other 4*d* perovskites are paramagnetic metals.

In Fig. 3, we plot the Néel temperatures for Tc and Mn band structures and several interaction strengths as a function of the coupling $g \equiv \mathcal{U}/\mathcal{U}_c$. The data are normalized with respect to the maximum value $T_N = T_N^*$ found for a given compound. Except at smallest g, where the details of the band structure become more important, the data fall on the same curve and can be described in terms of an universal function $T_N/W = f(\mathcal{U}/W, J/U)$. Moreover, the dependence on J/U (see the inset) is weak in the regime relevant for the two compounds. The maximum Néel temperature is found at a bit larger coupling than in the single-orbital Hubbard model but still close to the MIT. Close to the maximum, $SrTcO_3$ is found. On the localized side, the Néel temperature drops with increasing interactions, in accordance with $J_H \propto W^2/\mathcal{U}$, because $T_N \propto J_H S$ in this regime, and the Mn compound is found there. As $\mathcal{U}$ is diminished, the Néel temperature increases but more slowly than J_H does, because of the charge fluctuations which diminish the effective value of the local spin. T_N reaches a maximum where these fluctuations become substantial. LDA + DMFT is the method of choice to accurately describe materials such as $SrTcO_3$ which are in the regime where neither the fully localized nor the fully itinerant picture applies.

The maximal values of $T_N^* = W f(g^*, J/U)$ are thus reached for interaction $g^* \approx 1$. However, reducing the interaction strength in $SrMnO_3$ to g^* (Fig. 1, open circles) gives T_N, which still amounts only to about half of that found in $SrTcO_3$. Most of the additional increase can be attributed to the larger bandwidth of the Tc compound, setting the energy scale, as recognized also in Refs. [1,11]. The occurrence of large T_N of $SrTcO_3$ can thus be understood in two steps, schematically depicted by arrows in Fig. 1. First, T_N is maximized for a given band structure as $g \to g^* \approx 1$ (proximity to MIT), and, second, the change in the band structure given mostly by the bandwidth accounts for the rest of the enhancement. These observations provide important clues for engineering materials with robust magnetic properties.

It is instructive to consider the effect of an applied pressure, which increases the overall bandwidth and also reduces the coupling g. For $SrMnO_3$ both effects lead to an increase of T_N. In contrast, for $SrTcO_3$ the two effects largely cancel

each other. To substantiate this claim, we calculated T_N for both compounds for smaller volumes. Lattice parameters a were reduced by 1%, corresponding to about 5 GPa [24]. In $SrMnO_3$ we find a relative increase of T_N of 0.12, giving $-\alpha = d\log(T_N)/d\log V \approx 3.7$, which is somewhat smaller than the experimental value at small pressures [24]. For the same compression, T_N of $SrTcO_3$ remains *constant*. For larger compression with a diminished by 2%, $T_N/2$ *decreases* to 950 K corresponding to positive α. The qualitative conclusion that in $SrTcO_3$ the value of α is small follows from the proximity of the compound to the itinerant-to-localized transition and is thus robust against uncertainties ($\sim 20\%$) in the choice of interaction parameters.

The different position of the two materials on the $\mathcal{U}/\mathcal{U}_c$ diagram has also other consequences. The charge fluctuations $\delta N^2 = \langle N^2\rangle - \langle N\rangle^2$ are for $SrMnO_3$ small $\delta N^2 < 0.05$ as the material is situated well on the localized side. Instead, for $SrTcO_3$, we find large $\delta N^2 = 0.35$. Note that $\delta N^2 = 0.57$ for an atomic state $|\psi\rangle$, which consists of 2, 3, and 4 electron states with equal probability 1/3. The large value of the charge fluctuations for $SrTcO_3$ is further evidence that a localized Heisenberg model description [11] for these technetium compounds is questionable. These charge fluctuations explain also why the magnetic moment of Tc is smaller. If maximal spin compatible with charge fluctuations as in $|\psi\rangle$ is assumed, the local moment is reduced to $7/3\mu_B$, which would lead to a suppression of the moment by a factor of 7/9. In reality, the charge fluctuations in Tc are a bit smaller but still significant and crucial to explain the smaller magnetic moment of Tc. The paramagnetic moment for the two materials estimated from $\langle S_z^2\rangle$ above T_N is 2.7 for Tc and 3.8 for Mn compound. The paramagnetic magnetic moment of Mn is close to the maximal $S = 3/2$ moment 3.87, while for Tc charge fluctuations and related occurrence of states with smaller spins suppress the moment.

Finally, we turn to the delicate question of how to quantitatively determine the magnetic moment as measured by experiment. Magnetic moments obtained by different means are reported in Table I. Within LDA the moments are usually determined from the magnetization found in the muffin-tin spheres. This approach gives reasonable values for Mn compound, which only slightly underestimate experimental values, but fails badly for the Tc compound. This occurs because the larger 4d orbitals extend outside the muffin-tin spheres. Similar discrepancies with experiments are seen also if we calculate the magnetic moments within muffin-tin spheres in our approach. A less biased method is to determine the moment from the magnetization on the Wannier orbitals. If the small energy window orbitals ψ_m are used, these orbitals contain significant weight also on oxygens (due to covalency) and thus overestimate the experimental values. To obtain quantitative agreement with experiment, one must construct well-localized Wannier orbitals from an energy window including also oxygen bands. The magnetic moment found on these orbitals Ψ_m agrees with experiment within our precision. These results demonstrate unambiguously that (i) in $SrMnO_3$ the $\sim$15% suppression of the magnetic moment from maximal $3\mu_B$ is due to the covalency and (ii) in $SrTcO_3$ similar covalency effects are indeed seen but that (iii) most of the suppression of magnetic moment actually occurs due to the larger charge fluctuations in this much more itinerant compound.

TABLE I. (2nd–4th columns) Low-temperature staggered magnetic moments in units of μ_B, calculated within LDA + DMFT as obtained within muffin-tin (MT) spheres, on the extended Wannier function ψ_m, constructed without oxygen states, and on the localized Wannier function Ψ_m constructed by including all the oxygen states (see the text). These values are compared to LSDA (1st column) and experiment (last column).

Case	LSDA	MT	On ψ_m	On Ψ_m	Exp.
$SrTcO_3$	1.3	1.4	2.5	2.2	2.1 [1]
$SrMnO_3$	2.3	1.9	3.0	2.6	2.6 [7]

Conclusion.—In summary, we have calculated the properties of $SrTcO_3$ in the magnetic state with a combination of band-structure methods with the dynamical mean-field theory. We have shown that $SrTcO_3$ lies close to an itinerant-to-localized transition, which explains its high Néel temperature. Other 4d oxides do not have a half-filled t_{2g} shell and are thus further away from the transition, or they have distorted crystal structures, which reduces the bandwidth and suppresses the kinetic energy gain related to the formation of magnetic states. We have shown that the charge fluctuations in $SrTcO_3$ are large, which explain the smallness of the measured magnetic moment and implies that a purely localized (Heisenberg) description is not applicable. To put these results into perspective, we have analyzed the isostructural and isoelectronic 3d- $SrMnO_3$ within the same framework. This compound has a smaller bandwidth and lies further to the localized side which explains its much smaller Néel temperature and larger magnetic moment, despite similar covalency. The physical differences between the two materials imply very different pressure dependence of T_N, which is predicted to be weak for $SrTcO_3$. Taken together, these results help understand the occurrence of robust magnetism and may provide clues for designing magnetic materials.

We thank L. de' Medici, L. Pourovskii, and L. Vaugier for useful discussions. Support was provided by the Partner University Fund (PUF) and the Swiss National Foundation MaNEP program. M. A. acknowledges financial support by the Austrian Science Fund (FWF), Project No. F4103. J. M. acknowledges support from the Slovenian Research Agency under Contract No. P1-0044.

[1] E. E. Rodriguez, F. Poineau, A. Llobet, B. J. Kennedy, M. Avdeev, G. J. Thorogood, M. L. Carter, R. Seshadri, D. J. Singh, and A. K. Cheetham, Phys. Rev. Lett. **106**, 067201 (2011).

[2] G. J. Thorogood, M. Avdeev, M. L. Carter, B. J. Kennedy, J. Ting, and K. S. Wallwork, Dalton Trans. **40**, 7228 (2011).
[3] M. Avdeev, G. J. Thorogood, M. L. Carter, B. J. Kennedy, J. Ting, D. J. Singh, and K. S. Wallwork, J. Am. Chem. Soc. **133**, 1654 (2011).
[4] S. Nakatsuji, S. ichi Ikeda, and Y. Maeno, J. Phys. Soc. Jpn. **66**, 1868 (1997).
[5] A. Kanbayasi, J. Phys. Soc. Jpn. **41**, 1876 (1976).
[6] G. Cao, S. McCall, M. Shepard, J. E. Crow, and R. P. Guertin, Phys. Rev. B **56**, 321 (1997).
[7] T. Takeda and S. Ōhara, J. Phys. Soc. Jpn. **37**, 275 (1974).
[8] J. Hubbard and W. Marshall, Proc. Phys. Soc. London **86**, 561 (1965).
[9] The covalency occurs as the extended d orbitals hybridize strongly with oxygens, with strength of hybridization t_{pd}^2/Δ with t_{pd} the overlap and Δ the separation of oxygens from the t_{2g} states. While t_{pd} is larger in $SrTcO_3$ due to the larger spatial extension of $4d$ orbitals, the larger Δ compensates for this and the covalency of the two compounds is found to be comparable. See also R. Søndenå, P. Ravindran, S. Stølen, T. Grande, and M. Hanfland, Phys. Rev. B **74**, 144102 (2006).
[10] L. de' Medici, J. Mravlje, and A. Georges, Phys. Rev. Lett. **107**, 256401 (2011).
[11] C. Franchini, T. Archer, J. He, X.-Q. Chen, A. Filippetti, and S. Sanvito, Phys. Rev. B **83**, 220402 (2011).
[12] D. Bloch, J. Phys. Chem. Solids **27**, 881 (1966).
[13] M. Aichhorn, L. Pourovskii, V. Vildosola, M. Ferrero, O. Parcollet, T. Miyake, A. Georges, and S. Biermann, Phys. Rev. B **80**, 085101 (2009).
[14] M. Aichhorn, L. Pourovskii, and A. Georges, Phys. Rev. B **84**, 054529 (2011).
[15] P. Blaha, K. Schwarz, G. Madsen, D. Kvasnicka, and J. Luitz, *WIEN2k, An Augmented Plane Wave + Local Orbitals Program for Calculating Crystal Properties* (Technische Universitat Wien, Vienna, 2001), ISBN 3-9501031-1-2.
[16] M. Ferrero and O. Parcollet, "TRIQS: A Toolkit for Research in Interacting Quantum Systems," http://ipht.cea.fr/triqs.
[17] E. Gull, A. J. Millis, A. I. Lichtenstein, A. N. Rubtsov, M. Troyer, and P. Werner, Rev. Mod. Phys. **83**, 349 (2011).
[18] L. Boehnke, H. Hafermann, M. Ferrero, F. Lechermann, and O. Parcollet, Phys. Rev. B **84**, 075145 (2011).
[19] J. Mravlje, M. Aichhorn, T. Miyake, K. Haule, G. Kotliar, and A. Georges, Phys. Rev. Lett. **106**, 096401 (2011).
[20] J.-S. Kang, H. J. Lee, G. Kim, D. H. Kim, B. Dabrowski, S. Kolesnik, H. Lee, J.-Y. Kim, and B. I. Min, Phys. Rev. B **78**, 054434 (2008).
[21] A. I. Lichtenstein, M. I. Katsnelson, and G. Kotliar, Phys. Rev. Lett. **87**, 067205 (2001).
[22] M. J. Rozenberg, G. Kotliar, and X. Y. Zhang, Phys. Rev. B **49**, 10 181 (1994).
[23] See, e.g., L. de' Medici, Phys. Rev. B **83**, 205112 (2011).
[24] J.-S. Zhou and J. B. Goodenough, Phys. Rev. B **68**, 054403 (2003).